Biology of Reproduction, 2019, 101(5), 916–927
doi:10.1093/biolre/ioz148
Research Article
Advance Access Publication Date: 12 August 2019

OXFORD

Research Article

Role of lysyl oxidase like 1 in regulation of postpartum connective tissue metabolism in the mouse vagina†

Ali Borazjani[1], Bruna M. Couri[1,3], Mei Kuang[1], Brian M. Balog[1] and Margot S. Damaser[1,2,3,4,5,*]

[1]Department of Biomedical Engineering, Cleveland Clinic, Cleveland, OH, USA; [2]Department of Chemical & Biomedical Engineering, Cleveland State University, Cleveland, OH, USA; [3]Department of Obstetrics & Gynecology, Cleveland Clinic, Cleveland, OH, USA; [4]Glickman Urological & Kidney Institute, Cleveland Clinic, Cleveland, OH, USA; [5]Louis Stokes Veterans Affairs Medical Center, Cleveland, OH, USA

***Correspondence:** Department of Biomedical Engineering, The Cleveland Clinic, 9500 Euclid Avenue, ND20, Cleveland, OH 44195, USA. Tel: +1 216-444-1103; fax: +1 216-444-9198; E-mail: damasem@ccf.org

†**Grant support:** National Institutes of Health RO1 HD059859-01 and National Science Foundation Graduate Research Fellowship Grant # 1000139839.
‡**Conference Presentations:** Parts of this work were presented at The International Continence Society, October 20–24, 2014, Rio de Janeiro, Brazil; and Joint Meeting of the American Urogynecologic Society and International Urogynecological Association, July 22–26, 2014, Washington, DC, USA.

Received 19 August 2019; Revised 29 May 2019; Accepted 8 August 2019

Abstract

Pelvic organ prolapse (POP) in lysyl oxidase like-1 knockout *(Loxl1* KO) mice occurs primarily in parous mice and is rare in nulliparous mice. We determined the effect of *Loxl1* deficiency on postpartum regulation of connective tissue metabolism genes and degradative enzyme activity in the vagina at 20 days gestation or 4 h, 48 h, 7 days, 15 days, 25 days, 7 weeks, or 12 weeks postpartum. Nulliparous *Loxl1* KO and wildtype (WT) mice aged 11, 18, or 23 weeks were controls. Gene expression and enzyme activity were assessed using real-time quantitative reverse transcription PCR and fluorescein conjugated gelatin zymography, respectively. Parity, but not aging, had a significant influence on gene expression both with time postpartum and between KO and WT mice. *Mmp2*, *Timp1*, *Timp2*, *Timp3*, *Timp4*, *Col1a1*, *Col3a1*, *Acta2*, and *Bmp1* were differentially expressed between KO and WT mice. Correlational analysis of gene-gene pairs revealed 10 significant differences between parous KO and WT groups, 5 of which were due to lack of co-expression of *Bmp1* in KO mice. The overall enzyme activity that could be attributed to MMPs was significantly higher in WT compared to KO mice both 25 days and 12 weeks postpartum, and MMP activity was significantly lower 15 days and 25 days postpartum compared to KO nulliparous controls, but not WT. These findings suggest that *Loxl1* deficiency combined with parity has a significant impact on postpartum regulation of connective tissue metabolism, particularly as it relates to co-expression of *Bmp1* and altered proteolytic activity.

Summary Sentence

Loxl1 deficiency combined with parity has a significant impact on regulation of connective tissue metabolism in the vagina during puerperium, particularly as it relates to the co-expression of genes with *Bmp1*.

Key words: lysyl oxidase like 1, pelvic organ prolapse, extracellular matrix, vagina, postpartum, parity

Introduction

Pelvic organ prolapse (POP) is defined as the descent of the anterior, posterior, and/or apical vaginal compartment(s) with protrusion of one or more pelvic organs (e.g., bladder, uterus, posthysterectomy vaginal cuff, small bowel, or rectum) into the vagina [1]. Nearly half of all women in their fifth decade and beyond have evidence of POP on physical exam [2]. Symptomatic POP significantly affects quality of life in terms of discomfort, pain, and embarrassment that negatively impacts self-esteem, relationships, and sexual health [1].

POP is a highly prevalent condition accounting for nearly 1.5 million office visits annually [3]. Moreover, 12.6% of women will require surgical repair for POP by the age of 80 [4]. Despite the high incidence of POP, little is known regarding its pathophysiology. Therefore, current treatment options primarily involve surgical reconstruction, which does not address the underlying mechanisms of disease [5, 6]. Unfortunately, many of these surgeries, which aim to lift the prolapsed organs back into their anatomical position(s), have proven suboptimal with reoperation rates as high as 29.2% [7].

Collagens in pelvic connective tissues are composed primarily of collagen III (82%) and collagen I (13%) [8]. The major components of these proteins are encoded by collagen type I alpha 1 (Col1a1) and collagen type III alpha 1 (Col3a1) genes. Unlike collagens, elastic fibers are normally a stable component of the extracellular matrix (ECM) and turn over primarily during pregnancy and parturition [9]. The synthesis of elastic fibers requires tropoelastin (the monomeric form of elastin) and several cross-linking enzymes including lysyl oxidases and fibulins [10]. Lysyl oxidases, which cross-link both collagens and elastin, require activation by bone morphogenetic protein 1 (Bmp1), a matrix metalloproteinase that also cleaves the C-terminal propeptide of procollagen chains [11].

Lysyl oxidase like 1 (LOXL1) is known to be involved in the cross linking of tropoelastin monomers to generate mature elastin polymers. LOXL1 expression has been shown to be aberrant in patients with POP compared to those without POP [12–17]. Among other phenotypic characteristics, parous mice deficient in the *Loxl1* gene develop POP [18]. The biomechanical properties of the vagina and its support tissues are similar in nulliparous *Loxl1* KO and WT mice with the exception of ultimate load at failure, which is suggestive of mechanically weaker tissues [19]. Yet, unlike other mouse models of POP (e.g., *Fbln5* KO), nulliparous *Loxl1* KO mice rarely develop POP [20, 21]. In women, parity is a leading risk factor for POP, and likewise, parity drives POP development in *Loxl1* KO mice [21–23]. Less than 30% of primiparous mice develop POP by 12 weeks after delivery, whereas over 50% of mice allowed to breed to parity 3 develop POP by 12 weeks after first delivery, and over 80% develop POP by parity 5 [23]. Furthermore, like women, evading the process of parturition via Cesarean section (C-section) reduces but does not eliminate the risk of POP in these mice [24, 25]. Therefore, understanding the mechanisms of postpartum tissue recovery in *Loxl1* KO mice may lead to a better understanding of the pathophysiology of POP in parous women.

Given that repeat parity consistently results in POP development in these animals, we aimed to investigate the regulation of connective tissue metabolism genes around puerperium of parity 1. We hypothesized that the expression profile of genes involved in connective tissue metabolism is altered after vaginal delivery. To test this hypothesis, we determined expression levels of key matrix metalloproteinases (*Mmp2*, *Mmp9*, *Mmp12*), tissue inhibitors of metalloproteinases (*Timp1*, *Timp2*, *Timp3*, *Timp4*), and several genes involved in ECM synthesis including collagen type 1 (*Col1a1*), collagen type 3 (*Col3a1*), fibulin 5 (*Fbln5*), alpha smooth muscle actin (*Acta2*), and bone morphogenetic protein 1 (*Bmp1*) in the vagina of *Loxl1* KO and WT mice across a series of time points. We further evaluated degradative enzyme activity in these mice during and after puerperium.

Materials and methods

Animals

All animal protocols were approved by the Institutional Animal Care and Use Committee of the Cleveland Clinic. *Loxl1* KO mice ($n = 85$) were obtained from multiple breeding pairs in an already established colony in our laboratory. Female wild-type B6129F1/J mice ($n = 80$) were obtained from Jackson Laboratory (Cat #101043, Bar Harbor, MA, USA). The B6129SF1/J strain was chosen because *Loxl1* KO mice are of a similar genetic background.

Female mice were housed with male mice in single breeding pairs at 8–9 weeks of age and allowed to breed *ad libitum*. The pairs were allowed to cohabitate for 2 weeks at which time the males were removed from the cage. All animals were housed under a 12-h light cycle. We chose to study *Loxl1* KO mice because they provide a relevant animal model of POP in which development of POP is generally dependent on repeat parity and occurs many weeks postpartum [21]. Since the focus of this study was on gene expression during peurperium of parity 1, we did not observe POP in the mice in this study.

Experimental design

Given that the primary interest of this study was to assess postpartum changes in the vagina, we studied seven postpartum time points, one pregnant time point, and three ages of nulliparous mice as age-matched controls (Table 1). For all postpartum time points, the pups were removed immediately after birth (4 and 48 h postpartum groups) or within 24 h of birth (7 days, 15 days, 25 days, 7 weeks, and 12 weeks postpartum groups). The pregnant time point (~20 gestation) was included to assess connective tissue metabolism just prior to delivery. Female mice in our colony consistently deliver pups approximately 21 days after the date they are first set up with a male. For the pregnant time point, if vaginal plugs were not observed after cohabitation, then visibly pregnant mice were euthanized 20 days after the date a male was placed in the cage. Additionally, fetal crown-rump lengths were assessed to confirm late gestation pregnancy.

Table 1. Experimental design.

Time Point	KO	WT	mRNA	Enzyme Activity	Age Euthanized
Pregnant	$n = 7$	$n = 5$	X		11–12 weeks
4 h postpartum	$n = 6$	$n = 7$	X		11–12 weeks
48 h postpartum	$n = 7$	$n = 9$	X		11–12 weeks
7-Day postpartum	$n = 11$	$n = 12$	X		12–13 weeks
15-Day postpartum	$n = 7$	$n = 7$	X	X	13–14 weeks
25-Day postpartum	$n = 11$	$n = 8$	X	X	14–15 weeks
7-Week postpartum	$n = 8$	$n = 7$	X		18–19 weeks
12-Week postpartum	$n = 8$	$n = 7$	X	X	23–24 weeks
11-Week nulliparous	$n = 10$	$n = 10$	X	X	11–12 weeks
18-Week nulliparous	$n = 5$	$n = 4$	X		18–19 weeks
23-Week nulliparous	$n = 6$	$n = 5$	X	X	23–24 weeks
Subtotal	$n = 86$	$n = 81$			
Total	$n = 167$				

Note: *n* values represent the number of animals used for gene expression analyses. An *n* of 4–6 was used for enzyme activity assays at each time point.

To assess the effect of aging and to provide a nulliparous control arm to the study, *Loxl1* KO and WT nulliparous animals (aged 11, 18, and 23 weeks) were utilized.

At each time point, vaginas were harvested under anesthesia using 2.5% isoflurane in oxygen. Briefly, a midline abdominal incision was made, and the pubic symphysis was disarticulated. The bladder was dissected from surrounding tissues. The urethra was carefully dissected from the anterior vaginal wall using microsurgical instruments and a surgical microscope. The uterine horns were transected, and the cervix was used to apply traction to the vagina. The vagina was removed via incisions at the fornices and junction with the perineal skin. In the initial phases of the study, the vaginas were placed in cryovials on dry ice and stored in −80 °C following the procedure. However, preliminary analyses showed that half of each vagina was sufficient for extraction of mRNA and protein. Therefore, for most animals, the vagina was transected longitudinally to produce symmetrical halves—one half was allocated for mRNA and another half for protein extraction.

RNA isolation and cDNA generation

Frozen vagina specimen were placed a pocket of aluminum foil and placed in liquid nitrogen for approximately 15 s. Subsequently, a hemostat was used to pulverize the tissue within the foil. The crushed tissue was then placed in a microcentrifuge tube, and total RNA was isolated using an RNAqueous-4PCR kit (Cat. AM1914, Life Technologies, Grand Island, NY, USA) according to the manufacturer's protocol. Following DNase treatment and inactivation, the RNA concentration of each sample was determined using a NanoDrop ND-1000 Spectrophotometer (Thermo Scientific, Wilmington, DE, USA). Reverse transcription was performed using a High-Capacity cDNA Reverse Transcription Kit with RNase Inhibitor (Cat. 4374966, Life Technologies, Grand Island, NY, USA) in a 20-µL reaction volume with ∼300 ng of total RNA, random primers, dNTP mix, and 1 unit of MultiScribe reverse transcriptase at 25 °C for 10 min, 37 °C for 120 min, and 85 °C for 5 min.

Real-time quantitative reverse transcription PCR

Real-time quantitative reverse transcription PCR (qRT-PCR) was used to assess gene expression. Approximately, 30 ng of input cDNA was used in each 25 µL amplification reaction using TaqMan Gene Expression Master Mix (Cat. 4369016, Life Technologies, Grand Island, NY, USA) and TaqMan primer-probes (Table 2). Each reaction was carried out using the ABI 7500 Real-time PCR system (Life Technologies, Grand Island, NY, USA). The standard curve method was used to determine the relative amount of each target gene.

Table 2. Primer probes.

Gene Name	Gene Symbol	Assay ID
Matrix metalloproteinase 2	Mmp2	Mm00439498_m1
Matrix metalloproteinase 9	Mmp9	Mm00442991_m1
Matrix metalloproteinase 12	Mmp12	Mm00500554_m1
Tissue inhibitor of metalloproteinase 1	Timp1	Mm00441818_m1
Tissue inhibitor of metalloproteinase 2	Timp2	Mm00441825_m1
Tissue inhibitor of metalloproteinase 3	Timp3	Mm00441826_m1
Tissue inhibitor of metalloproteinase 4	Timp4	Mm01184417_m1
Collagen type I alpha 1	Col1a1	Mm00801666_g1
Collagen type III alpha 1	Col3a1	Mm01254476_m1
Fibulin 5	Fbln5	Mm00488601_m1
Bone morphogenetic protein 1	Bmp1	Mm00802220_m1
Smooth muscle alpha actin 2	Acta2	Mm01546133_m1
18s Ribosomal RNA	18 s	4319413E

Note: All primer probes purchased from Life Technologies, Inc.

Protein extraction

Protein was extracted from vaginal specimen by first pulverizing tissues using aluminum foil and liquid nitrogen as detailed above. Subsequently, the pulverized sample was placed in a microcentrifuge tube and 100 µL of homogenization buffer per 10 mg tissue (wet weight). The homogenization buffer consisted of 10 mM Tris–HCl (pH 7.4), 150 mM NaCl, 10 mM $CaCl_2$, and 0.1% Triton-X 100. Following addition of the homogenization buffer, the samples were placed on ice and homogenized using a tissue grinder and microcentrifuge pestle. The samples were then centrifuged at 10 000 × *g* for 30 min at 4 °C in a microcentrifuge. The supernatant was collected and frozen at −80 °C until testing.

Enzyme activity assay

The BCA protein quantification assay (Cat # 23225, Pierce Biotechnology, Thermo Scientific, Rockford, IL, USA) was used to quantify the protein concentration of each sample according to manufacturer's instructions. Bovine serum albumin in phosphate buffered saline was used as the standard curve. Absorbance was read at 562 nm, and a second-order polynomial fit was used to extrapolate protein concentrations. For analysis of enzyme activity, the EnzChek Gelatinase/Collagenase Assay Kit (Cat # E-12055, Molecular Probes, Eugene, OR, USA) was used according to manufacturer's instructions. This assay utilizes a proprietary fluorescein conjugated gelatin substrate (DQ gelatin), whose fluorescence is quenched in the undigested form. Upon digestion with gelatinases and collagenases, the substrate yields highly fluorescent peptides. The change in fluorescence is proportional to proteolytic activity.

To determine the optimal incubation time, concentration of DQ gelatin, and input protein, a series of preliminary assays were performed. Incubation times ranging from 4 to 24 h, DQ gelatin concentrations ranging from 6.25 to 75 µg/mL per reaction, and input protein amounts ranging from 2 to 30 µg per 200 µL reaction were tested in an optimization matrix. The combination with the optimal signal-to-noise ratio was chosen as follows: incubation time, 24 h; DQ gelatin concentration, 100 µg/mL; input protein, 15 µg/200 µL reaction.

To determine the differential contribution of MMPs and serine proteases on overall proteolytic activity, parallel assays using ethylenediaminetetraacetic acid (EDTA) and phenylmethylsulfonyl fluoride (PMSF) were performed. EDTA is a well-established inhibitor of MMPs and was used at a final concentration of 10 mM per reaction. PMSF, which is a broad-spectrum serine protease inhibitor, was used at a final concentration of 2.2 mM per reaction. Background fluorescence values were obtained from appropriate blank reactions (i.e., reaction buffer only, reaction buffer + EDTA, reaction buffer + PMSF). Fluorescence without inhibitors, fluorescence in the presence of inhibitors, and percent MMP and serine protease activity were reported. The latter was calculated using the following equations:

$$\%\text{MMP activity} = \left(\frac{F_{\text{no inhibitors}} - F_{\text{EDTA}}}{F_{\text{no inhibitor}}}\right) \times 100$$

$$\%\text{Serine protease activity} = \left(\frac{F_{\text{no inhibitors}} - F_{\text{PMSF}}}{F_{\text{no inhibitor}}}\right) \times 100$$

where $F_{\text{no inhibitors}}$ is the fluorescence without any inhibitors, F_{EDTA} is the fluorescence in the presence of EDTA, and F_{PMSF} is the fluorescence of PMSF.

Statistical analyses

All statistical analyses were performed using GraphPad Prism Version 6.05 (GraphPad Software Inc., La Jolla, CA, USA). To determine the effect of *Loxl1* deficiency, we compared KO and WT groups at each time point using one-way ANOVA followed by the Holm-Sidak posthoc test. To determine changes in gene expression as a function of age, we compared nulliparous mice in various age groups (11, 18, and 23 weeks) in *Loxl1* KO and WT mice using one-way ANOVA followed by the Holm-Sidak posthoc test. In addition to determining significant differences in overall expression levels of each gene between KO and WT mice, we also investigated the correlational relationships between these genes [26]. To identify genes that are co-expressed (i.e., linearly associated) Pearson's correlations analysis was performed between genes within each group. To determine whether correlation coefficients in KO mice were significantly different from WT mice, the Fisher r-to-z transformation was performed and z was applied using a normal distribution to determine *P*-values [27]. To determine whether the magnitude of effect of one gene on another gene was significantly different in KO mice compared to WT mice, linear regression analysis was performed between genes within each group. Preliminary analyses showed that the average distance between points and the regression line was proportional to values on the *Y*-axis. Therefore, the linear regression was weighted by $1/Y^2$. To determine whether regression slopes in KO mice were significantly different from WT mice, *z* was computed as the difference between KO and WT slopes divided by the standard error of the difference between the slopes. Subsequently, *z* was applied using a *t*-distribution to determine *P*-values [28].

GraphPad Prism's ROUT (Robust regression and Outlier removal) algorithm, which is based on methods developed by Motulsky and Brown [29], was used to identify potential outliers prior to statistical analyses. For assessment of relative gene expression, the ROUT coefficient (*Q*) was set at 1% (at least 99% of the identified outliers will be real be outliers). This identified outliers at each time point for each group. One-way ANOVA, Pearson's correlation, and linear regression analyses were performed on data once outliers were removed. $P < 0.05$ was used to determine statistical significance. Data are presented as mean ± standard error.

Table 3. Demographics.

	KO	WT	*P*-Value
Age at breeding (weeks)[a]	8.5 ± 0.6	8.5 ± 0.7	0.882
Age at delivery (weeks)[b]	11.7 ± 0.6	11.4 ± 0.6	0.057
Gestation (days)	21.6 ± 1.4	20.7 ± 1.6	0.003
Number of pups/delivery[c]	7.4 ± 1.7	8 ± 1.4	0.044
Animal weights (g)[d]			
48 h postpartum	19.9 ± 0.7	21.9 ± 0.8	0.172
7-Day postpartum	19.6 ± 1.2	21.5 ± 0.9	0.172
25-Day postpartum	19.9 ± 0.4	24 ± 1.9	0.004
7-Week postpartum	19.1 ± 1.1	22.5 ± 0.8	0.001
12-Week postpartum	20.7 ± 1.3	22.4 ± 2.4	0.172
11-Week-old nulliparous	16.3 ± 0.5	18.5 ± 1.1	0.172
18-Week-old nulliparous	18.7 ± 0.7	23.5 ± 1	<0.001
23-Week-old nulliparous	18.4 ± 1	27.6 ± 4.8	<0.0001
		Overall *P*-value	<0.0001

Note: Data presented as mean ± standard deviation. A two-tailed *t*-test was used to assess significance with $P < 0.05$ indicating a significant difference between groups.
[a]Age of animals at the date of initial male/female cohabitation.
[b]Age of animals at date of delivery.
[c]Includes stillborn and live pups.
[d]Weight of animal prior to euthanasia.

Results

A total of 167 mice were used for this study. Demographics are presented in Table 3. Loxl1 KO mice delivered approximately 1 day later than WT mice ($P = 0.003$) and, the litter size of *Loxl1* KO mice was significantly smaller than WT mice ($P = 0.044$). Overall, WT mice were heavier than *Loxl1* KO mice at each time point ($P < 0.0001$).

Aging did not play a significant role in gene expression at the studied time points with the exception of *Bmp1*, which was upregulated in 18-week-old nulliparous WT mice compared to nulliparous 11-week-old WT mice (Figures 1 and 2).

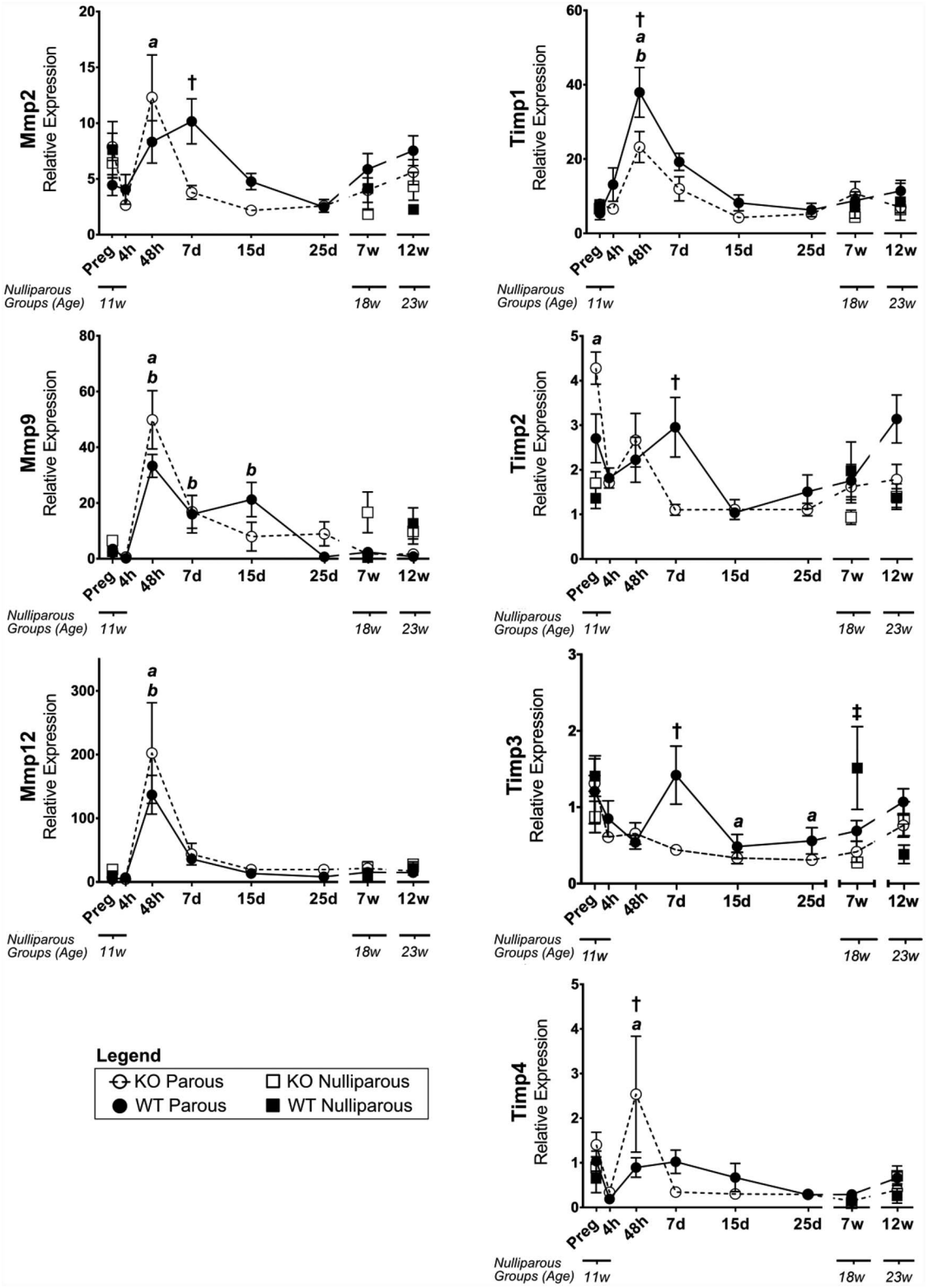

Figure 1. Relative *Mmp* and *Timp* gene expression levels in lysyl oxidase like-1 (*Loxl1*) knockout (KO) and wildtype (WT) mice at several time points postpartum and in pregnant (Preg) and age-matched nulliparous mice. Symbols represent mean ± standard error of data from $n = 5$–10 mice. $P < 0.05$ considered statistically significant (one-way ANOVA with Holm-Sidak posthoc test). WT vs KO statistical significance indicators: †Parous WT vs Parous KO; ‡Nulliparous WT vs Nulliparous KO; [a]Nulliparous KO vs Parous KO; [b]Nulliparous WT vs Parous WT. Nulliparous KO vs Nulliparous KO statistical significance indicators: [c]11 weeks vs 18 weeks, [d]11 weeks vs 23 weeks, and [e]18 weeks vs 23 weeks. Nulliparous WT vs Nulliparous WT statistical significance indicators: [f]11 weeks vs 18 weeks, [g]11 weeks vs 23 weeks, and [h]18 weeks vs 23 weeks.

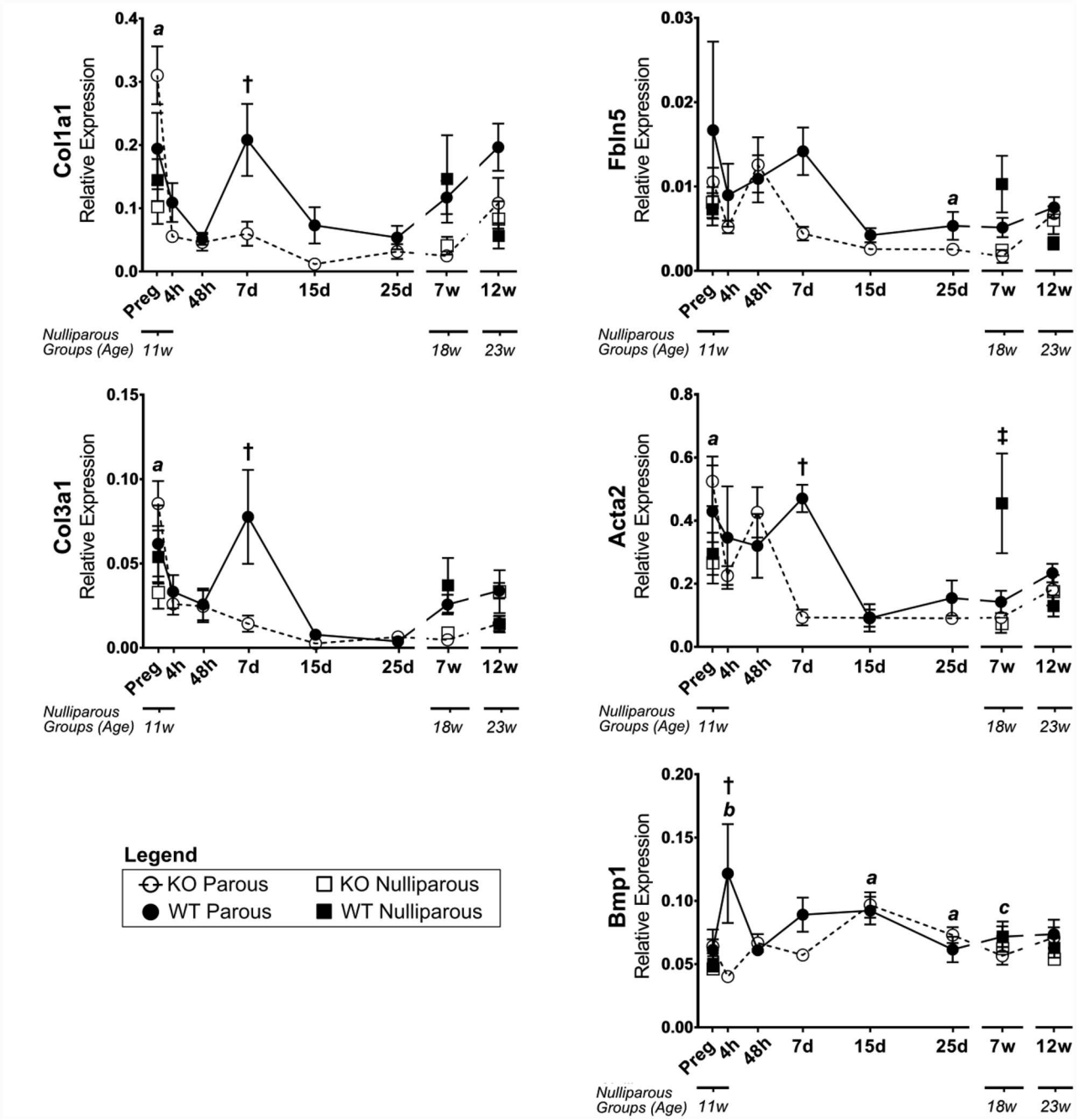

Figure 2. Relative gene expression levels of Col1a1, Col3a1, Fbln5, Acta2, and Bmp1 in lysyl oxidase like-1 (*Loxl1*) knockout (KO) and wildtype (WT) mice at several time points postpartum and in pregnant (Preg) and age-matched nulliparous mice. Symbols represent mean ± standard error of data from $n = 4$–10 mice. $P < 0.05$ considered statistically significant (one-way ANOVA with Holm-Sidak posthoc test). WT vs KO statistical significance indicators: †Parous WT vs Parous KO; ‡Nulliparous WT vs Nulliparous KO; [a]Nulliparous KO vs Parous KO; [b]Nulliparous WT vs Parous WT. Nulliparous KO vs Nulliparous KO statistical significance indicators: [c]11 weeks vs 18 weeks, [d]11 weeks vs 23 weeks, and [e]18 weeks vs 23 weeks. Nulliparous WT vs Nulliparous WT statistical significance indicators: [f]11 weeks vs 18 weeks, [g]11 weeks vs 23 weeks, and [h]18 weeks vs 23 weeks.

Mmp2, *Timp1*, *Timp2*, *Timp3*, *Timp4*, *Col1a1*, *Col3a1*, *Acta2*, and *Bmp1* were all differentially expressed between KO and WT animals (Figures 1 and 2). Beginning with the earliest time points, *Bmp1* was downregulated 4 h postpartum in KO compared to WT mice. Subsequently, *Timp1* was downregulated 48 h postpartum, whereas *Timp4* was upregulated at the same time point in KO compared to WT mice. Seven days postpartum, *Mmp2*, *Timp2*, *Timp3*, *Col1a1*, *Col3a1*, and *Acta2* were downregulated in KO compared to WT mice. However, there were no differences between KO and WT mice 15 days, 25 days, 7 weeks, or 12 weeks postpartum. Among

nulliparous animals, only *Timp3* and *Acta2* were upregulated in 18-week-old nulliparous WT mice compared to age-matched nulliparous KO mice.

There was a distinct pattern of upregulation in *Mmp9*, *Mmp12*, *Timp1*, and *Bmp1* beginning at 4 or 48 h followed by a return to prepregnancy expression levels by 25 days postpartum in WT mice (Figures 1 and 2). This pattern was preserved in KO mice with the exception of Bmp1, which was not upregulated until 15 days postpartum. There were no differences between 7 or 12 weeks postpartum mice and their age-matched nulliparous mice (18 and 23 weeks age, respectively) in any of the genes assessed.

Compared to 11-week-old nulliparous mice, *Timp2*, *Col1a1*, *Col3a1*, and *Acta2* were upregulated at 20 days gestation (G20D) in KO but not WT mice. However, *Mmp9*, *Mmp12*, and *Timp1* were upregulated 48 h postpartum in both WT and KO mice. *Mmp2* and *Timp4* were upregulated 48 h in KO, but not WT mice. *Mmp9* was upregulated 7 and 15 days postpartum in WT, but not KO mice. Fifteen and 25 days postpartum, *Timp3* was downregulated in KO mice, whereas *Bmp1* was upregulated compared to 11-week-old nulliparous mice (Figures 1 and 2). Although *Fbln5* was downregulated 25 days postpartum in KO mice, there were no other significant differences either within groups or between groups in its gene expression.

Pearson's correlation analysis revealed multiple co-expressed genes in both parous and nulliparous mice (Figure 3). The total number of statistically significant correlations was higher in parous animals than in nulliparous animals (KO mice: 33 nulliparous vs 39 parous; WT mice: 27 nulliparous vs 45 parous).

As was observed with analyses of relative gene expression levels, parity resulted in increased aberrant co-expression of genes in KO compared to WT mice (Figure 4). In total, 16 significant differences were identified among correlation coefficients, the majority of which occurred only in parous animals. Of the 10 significant differences observed in parous animals, 5 involved *Bmp1 (*Figure 4A*)*. These specific gene–gene pairs included *Bmp1-Timp3*, *Bmp1-Col1a1*, *Bmp1-Col3a1*, *Bmp1-Fbln5*, and *Bmp1-Acta2*. These five differences were all a result of a lack of co-expression with *Bmp1* in KO mice (Figure 3A). Analyses of linear regression lines showed that the slopes between these genes were all significantly higher in WT compared to KO mice, with the exception of *Bmp1-Acta2* (Figure 4B). Overall, the following gene–gene pairs were found to have both significantly different correlation coefficients and slopes: *Bmp1-Timp3* (parous only), *Bmp1-Col1a1* (parous and nulliparous), *Bmp1-Col3a1* (parous only), *Bmp1-Fbln5* (parous only), *Bmp1-Acta2* (nulliparous only), *Timp1-Mmp9* (nulliparous only), and *Timp1-Mmp12* (nulliparous only).

There were no differences in overall collagenase/gelatinase activity between *Loxl1* KO and WT mice (Figure 5A). There was significantly more enzyme activity in 15 days postpartum WT mice compared to nulliparous WT controls. As a result, there was also significantly more enzyme activity in the presence of EDTA and PMSF in 15 days postpartum WT mice compared to nulliparous WT controls (Figure 5B and C). Overall, enzyme activity steadily decreased from 15 days to 12 weeks postpartum in WT mice (Figure 5A). In contrast, this trend was not observed in KO mice. The percentage of overall enzyme activity that could be attributed to MMPs was significantly higher in WT compared to KO mice at both 25 days ($69.9 \pm 4.4\%$ vs $39.1 \pm 6.1\%$, $P = 0.003$) and 12 weeks postpartum ($75.4 \pm 5.8\%$ vs $50.1 \pm 8.1\%$, $P = 0.006$) (Figure 5D). Moreover, percent MMP activity was significantly lower 15 and 25 days postpartum compared to nulliparous controls in KO, but not in WT mice (Figure 5D). There were no significant differences between groups or time points with regards to percent serine protease activity.

Discussion

Epidemiological studies suggest that the pathologic processes leading to POP likely begin with pregnancy and vaginal childbirth [1]. Intriguingly, some women, even after several vaginal deliveries, never develop the disorder, while others may be afflicted after a single delivery. Furthermore, evading the process of parturition via Cesarean section may not completely eliminate the risk of POP [30].

ECM remodeling of the pelvic soft tissues occurs during the peripartum period, and is likely modulated by connective tissue degradative enzymes including matrix metallopeptidases (MMPs) and their tissue inhibitors (TIMPs) [31–34]. Case-controlled studies investigating alterations in connective tissue metabolism (as evident by changes in MMPs and TIMPs) have found significant differences between patients with POP compared to those without POP [35].

Although a few studies that investigate the regulation of connective tissue metabolism genes during pregnancy and puerperium in the mouse vagina have been performed [31, 36], our study was the first to investigate both *Mmps* and *Timps*, as well as key genes involved in connective tissue synthesis (i.e., *Col1a1*, *Col3a1*, *Fbln5*, and *Acta2*). We found that several genes (including *Mmp9*, *Mmp12*, *Timp1*, and *Bmp1*) demonstrated a distinct pattern characterized by upregulation in gene expression during the early postpartum period followed by a return to prepregnancy state. This is consistent with a previous study by Drewes et al. that found a surge in elastic fiber synthesis and *Mmp* gene expression following delivery [36]. In our study, the earliest regulated event was evident 4 h postpartum, when *Bmp1* was significantly upregulated compared to nulliparous controls in WT mice. This finding was not observed in KO mice, until at least 15 days postpartum. Given that BMP1 is required for activation of LOXL1, which is required for physiologic elastic fiber repair, it is plausible that the lack of upregulation in KO mice may be due to a decreased demand for Bmp1 [11, 18, 37].

In addition to activation of LOXL1, BMP1 is known to play a significant role collagen synthesis [38, 39]. Therefore, aberrant regulation of *Bmp1* could impact the regulation of other connective tissue metabolism genes. Indeed, we found that of the 10 significant differences observed between correlational analysis of gene–gene pairs, 5 involved *Bmp1*. These specific gene–gene pairs included *Bmp1-Timp3*, *Bmp1-Col1a1*, *Bmp1-Col3a1*, *Bmp1-Fbln5*, and *Bmp1-Acta2*. Moreover, all these differences were a result of a lack of co-expression of *Bmp1* in KO mice. These results were further confirmed by linear regression analyses, which showed that the slopes between these genes were all significantly higher in WT mice compared to KO mice, with the exception of *Bmp1-Acta2*.

Further comparisons of KO and WT mice revealed differential expression of multiple genes in addition to *Bmp1*. Seven days postpartum, WT mice demonstrated a pattern of upregulation involving 6 of the 12 genes we investigated. Specifically, *Mmp2*, *Timp2*, *Timp3*, *Col1a1*, *Col3a1*, and *Acta2* were all upregulated in WT compared to KO mice. Interestingly, these are most of the same genes that were aberrantly correlated with *Bmp1*. Overall, these findings are consistent with the hypothesis that *Loxl1* deficiency results in a decreased demand for *Bmp1* and that this results in aberrant downstream regulation of other connective tissue metabolism genes.

The specific finding that *Acta2* is upregulated in concert with *Col1a1* and *Mmp2* is suggestive of the phenomena of fibroblast

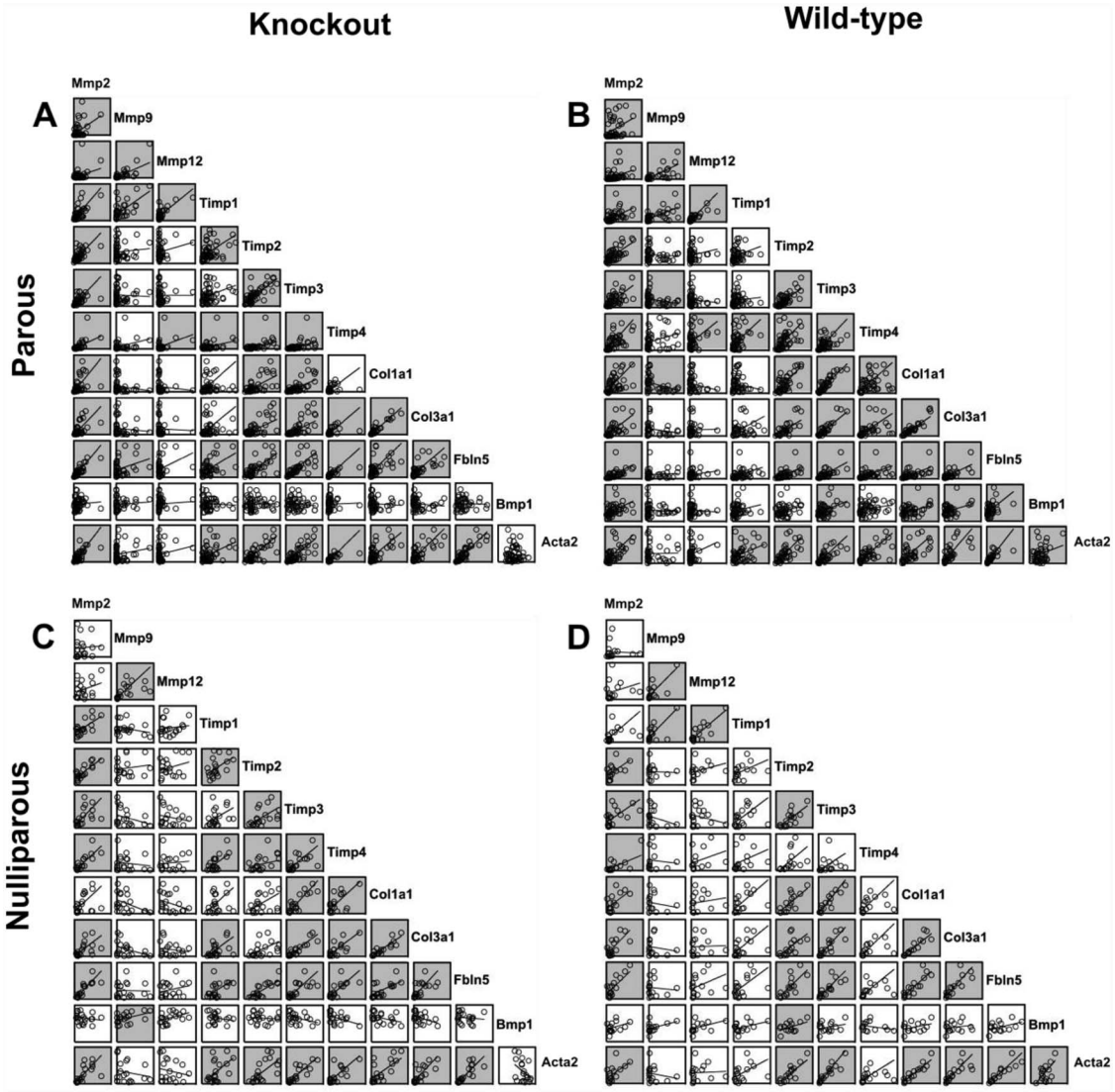

Figure 3. Correlation matrices and linear regression analysis. Correlation matrices with scatter plots and regression lines are presented in panels A–D. Panels A, B, C, and D illustrate gene–gene correlations between genes in parous KO mice, parous WT mice, nulliparous KO mice, and nulliparous WT mice, respectively. Shaded boxes indicate a significant Pearson's correlation coefficient ($P < 0.05$) between the specified gene–gene pair.

activation. Fibroblasts have been shown to acquire an activated phenotype in response to stimuli induced by tissue injury [40]. These stimuli include transforming growth factor-β (TGFβ), epidermal growth factor (EGF), platelet-derived growth factor (PDGF), and fibroblast growth factor 2 (FGF2) [40, 41]. Activated fibroblasts synthesize large amounts of ECM components, express α-smooth-muscle actin (e.g., *Acta2*), and upregulate production of MMPs, including *Mmp2* [41, 42]. Overall, these changes enable alterations in ECM composition and turnover [41].

Given that the primary markers of an activated fibroblast include expression of alpha smooth muscle, COL1, and Mmp2 [42–45], we propose that connective tissue recovery in *Loxl1* KO mice could be impeded by the lack of fibroblast activation. Given the similarity between *Loxl1* KO mice and women with regards to the association of parity and POP, it is possible that a similar defect in postpartum recovery occurs in women that go on to develop POP. Moreover, this observation presents a potential promising prophylactic and/or therapeutic approach for the prevention of POP. Nonetheless, these preliminary *in vivo* findings merit further investigation.

Our study was strengthened by the inclusion of multiple nulliparous time points (ages 11–23 weeks), which allowed us to investigate the effect of aging on gene expression. We found that *Bmp1* was upregulated in 18-week-old WT mice compared to 11-week-old WT mice. We found no other significant differences across nulliparous time points in any of the other genes, suggesting that aging did not play a significant role in gene expression at the selected time points and that the majority of ECM enzyme regulation is parity dependent. Since mice pups are ready to wean by 3–4 weeks of age and dams that are allowed to breed ad libitum deliver their next litter soon after weaning of pups [46, 47], it is probable that the process of connective tissue recovery during puerperium in mice is complete by approximately 4 weeks postpartum. In support of this, we found no differences in gene expression of mice 7 and 12 weeks postpartum compared to age-matched controls. Therefore, our results indicate that connective tissue metabolism at the level of transcription is

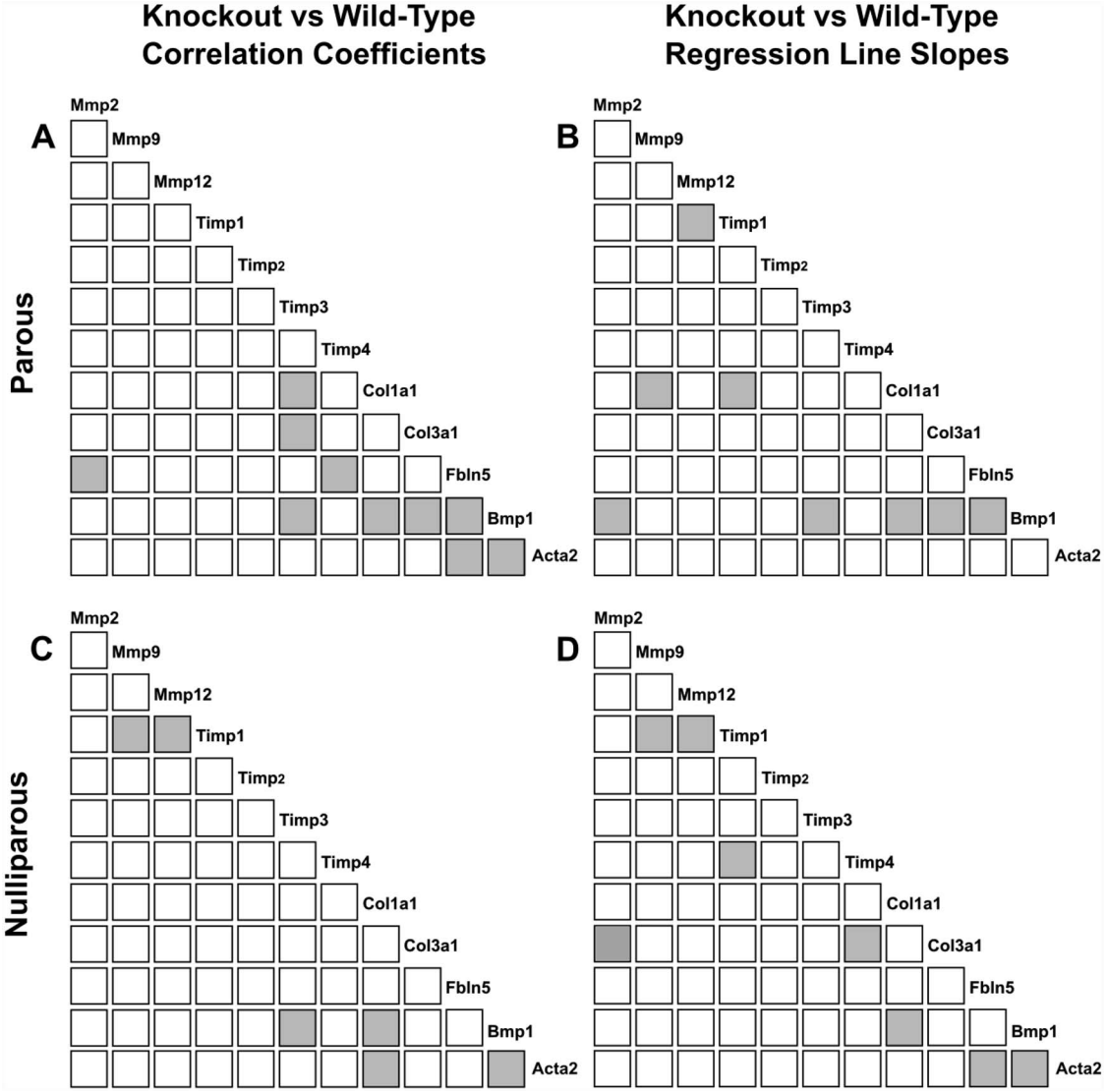

Figure 4. Statistical comparisons of correlation coefficients and regression lines. Comparisons between parous KO and parous WT correlation coefficients (using Fisher *r*-to-*z* transformation) are presented in panel A and between nulliparous KO and nulliparous WT in panel C. Comparisons between parous KO and parous WT regression line slopes are presented in panel B and between nulliparous KO and nulliparous WT in panel D. Shaded boxes indicate significant difference ($P < 0.05$) in correlation coefficients or regression line slopes between KO and WT.

highly regulated during gestation and puerperium, but relatively homeostatic following the recovery period.

Some case-controlled studies comparing women with and without POP have suggested alterations in connective tissue degradative activity in women with POP compared to women without POP [48, 49]. Although the design of such studies precludes the ability to establish causality, a study using *Fbln5* KO mice has shown that vaginal protease activity precedes POP [20]. Moreover, studies using WT mice have found that MMP2 and MMP9 activity is significantly increased 48 h postpartum compared to nulliparous controls [31]. Given these findings, we hypothesized that changes observed in gene expression of *Loxl1* KO mice would directly or indirectly result in increased long-term connective tissue degradation.

A limitation of this study is that protein expression levels and localization of expression of the target genes were not assessed. However, since this is the first study investigating the pathophysiology of prolapse in *Loxl1* KO mice at the molecular level, we aimed for this study to be exploratory in nature. Focusing at the transcriptional level enabled us to include additional time points as well as analysis of a variety of genes known to play a role in both ECM synthesis and degradation. A strength of our study is the utilization of robust correlational analyses in addition to assessment of gene expression levels. Differences in gene–gene co-expression were of particular importance to us since co-expressed genes are likely controlled by the same transcriptionally regulatory pathway and are functionally related [50–52]. Another limitation of this study is that we did not investigate tissues other than the vagina to determine whether changes observed are specific to the vagina or systemic. However, our aim was to study changes in pelvic connective tissue metabolism, and therefore, we chose to focus on the vagina because it is contiguous with the endopelvic fascia and is commonly used as a surrogate for studies investigating pelvic organ support tissues [35, 53].

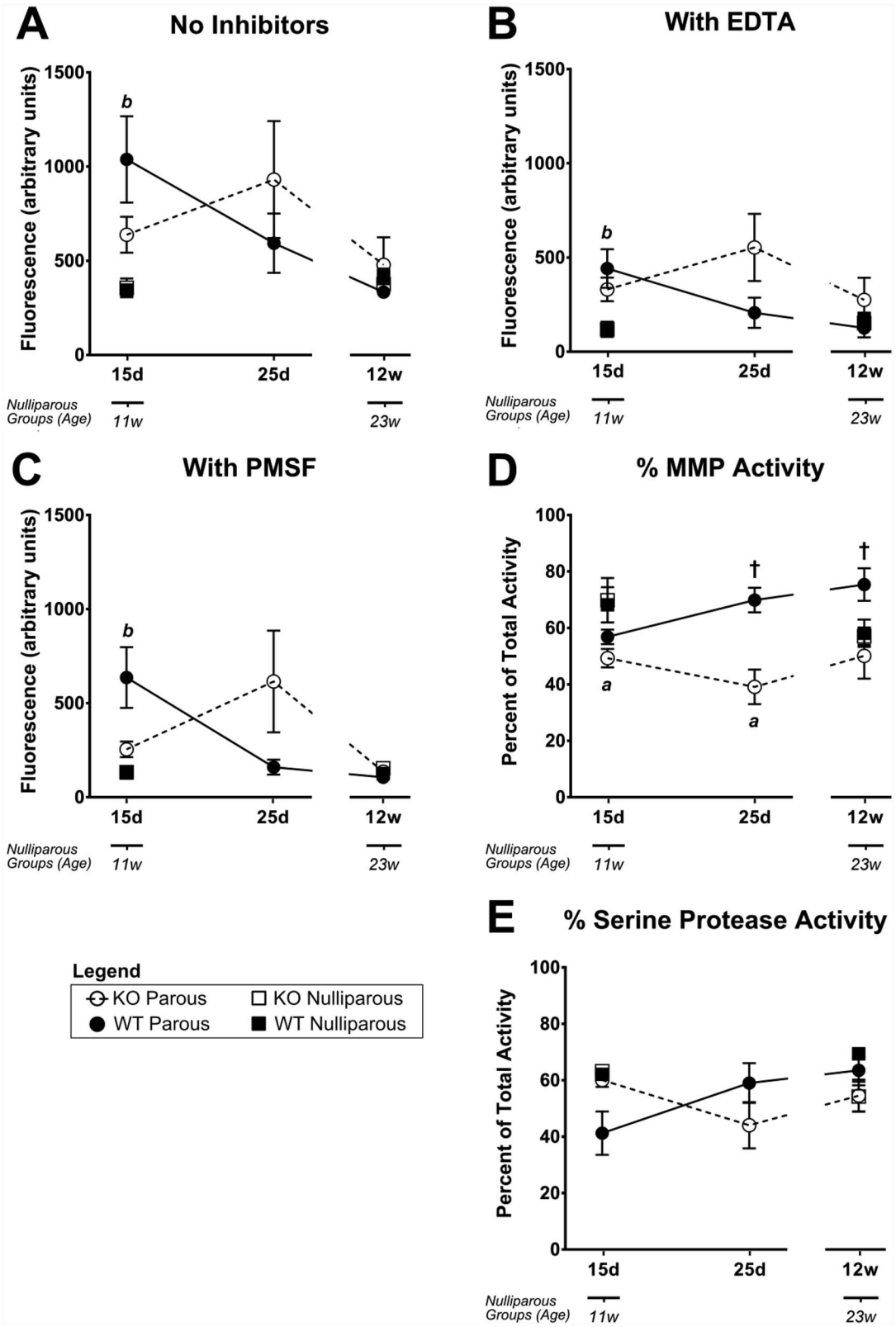

Figure 5. Collagenase/gelatinase activity assay in lysyl oxidase like-1 (*Loxl1*) knockout (KO) and wildtype (WT) mice at several time points postpartum and in pregnant (Preg) and age-matched nulliparous mice. Symbols represent mean ± standard error of data from $n = 4$–6 mice. (A) Overall enzyme activity, (B) enzyme activity in the presence of 10 mM EDTA, (C) enzyme activity in the presence of 2.2 mM PMSF, (D) percent of overall enzyme activity that can be attributed to MMPs, and (E) percent of overall enzyme activity that can be attributed to serine proteases. Summation of MMP and serine protease activities may be greater than 100% due to cross inhibition of collagenases/gelatinases by EDTA and PMSF. $P < 0.05$ considered statistically significant (one-way ANOVA with Holm-Sidak posthoc test). WT vs KO statistical significance indicators: [†]Parous WT vs Parous KO; [‡]Nulliparous WT vs Nulliparous KO; [a]Nulliparous KO vs Parous KO; [b]Nulliparous WT vs Parous WT. Nulliparous KO vs Nulliparous KO statistical significance indicators: [c]11 weeks vs 18 weeks, [d]11 weeks vs 23 weeks, and [e]18 weeks vs 23 weeks. Nulliparous WT vs Nulliparous WT statistical significance indicators: [f]11 weeks vs 18 weeks, [g]11 weeks vs 23 weeks, and [h]18 weeks vs 23 weeks.

We chose to use the EnzCheck Collagenase/Gelatinase Assay, which is claimed to be capable of measuring proteolytic activity of most, if not all, collagenases and gelatinases. In contrast to our hypothesis, we found no differences in overall collagenase/gelatinase activity between *Loxl1* KO and WT mice during late puerperium (i.e., 15 and 25 days) or long term (i.e., 12 weeks postpartum). However, the percentage of overall proteolytic activity that could be attributed to MMPs was significantly higher in WT compared to KO mice 25 days and 12 weeks postpartum, suggesting that although there are no differences in overall proteolytic activity, the differential composition of proteolytic activity between KO and WT mice may result in pathophysiological changes long after delivery.

Such alterations in proteolytic activity can result in cleavages that generate different bioactive peptides or matrikines, bioactive ligands derived from ECM proteins [54, 55]. Indeed, matrikines released following MMP cleavage have been shown to be involved in a variety of physiological and pathophysiological processes including the ability to interact with elastin-binding protein [56–58], promote ECM synthesis [58, 59], stimulate proliferation [58, 60], and demonstrate chemotactic activity [58, 61, 62]. Therefore, the altered long-term proteolytic activity we observed as a result of *Loxl1* deficiency may have profound pathophysiological effects. These results are of particular interest given that alterations in proteolytic activity were only observed in parous *Loxl1* KO mice and not nulliparous mice, which rarely develop POP.

In conclusion, we showed that parity, but not aging, had a significant influence on gene expression both with time and between KO and WT mice. Moreover, since prolapse development in *Loxl1* KO mice is heavily dependent on parity, the differential expressions observed between KO and WT mice is indicative of the pathophysiology of prolapse in this animal model. Correlational analyses revealed that *Bmp1* may play a significant role in this pathophysiological mechanism through its involvement with *Timp3*, *Col1a1*, *Col3a1*, *Fbln5*, and *Acta2*. Furthermore, our finding showing that *Mmp2*, *Col1a1*, *Col3a1*, and *Acta2* are upregulated at 7 days in WT compared to KO mice is indicative of a diminished fibroblast activation response in KO mice. Overall, we found no differences in gene expression between parous KO and WT mice between 15 days and 12 weeks postpartum. However, we did observe alterations in proteolytic activity between the groups at 25 days and 12 weeks postpartum, suggesting tissue remodeling during the early postpartum period may have long-term effects on proteolytic activity. Given that parity is the greatest risk factor for prolapse in *Loxl1* KO mice and women, our results provide insight into the potential mechanisms of disease in women.

References

1. Jelovsek JE, Maher C, Barber MD. Pelvic organ prolapse. *Lancet* 2007; **369**:1027–1038.
2. Swift SE. The distribution of pelvic organ support in a population of female subjects seen for routine gynecologic health care. *Am J Obstet Gynecol* 2000; **183**:277–285.
3. Sung VW, Raker CA, Myers DL, Clark MA. Ambulatory care related to female pelvic floor disorders in the United States, 1995–2006. *Am J Obstet Gynecol* 2009; 201: 508 e501–506.
4. Wu JM, Matthews CA, Conover MM, Pate V, Jonsson FM. Lifetime risk of stress urinary incontinence or pelvic organ prolapse surgery. *Obstet Gynecol* 2014; **123**:1201–1206.
5. DeLancey JO. The hidden epidemic of pelvic floor dysfunction: achievable goals for improved prevention and treatment. *Am J Obstet Gynecol* 2005; **192**:1488–1495.
6. Gomelsky A, Penson DF, Dmochowski RR. Pelvic organ prolapse (POP) surgery: the evidence for the repairs. *BJU Int* 2011; **107**:1704–1719.
7. Olsen AL, Smith VJ, Bergstrom JO, Colling JC, Clark AL. Epidemiology of surgically managed pelvic organ prolapse and urinary incontinence. *Obstet Gynecol* 1997; **89**:501–506.
8. Moalli PA, Talarico LC, Sung VW, Klingensmith WL, Shand SH, Meyn LA, Watkins SC. Impact of menopause on collagen subtypes in the arcus tendineous fasciae pelvis. *Am J Obstet Gynecol* 2004; **190**:620–627.
9. Mecham R, Heuser J. The elastic fiber. In: Hay E (ed.), *Cell Biology of Extracellular Matrix*. New York: Springer US; 1991: 79–109.
10. Wagenseil JE, Mecham RP. New insights into elastic fiber assembly. *Birth Defects Res C Embryo Today* 2007; **81**:229–240.
11. Uzel MI, Scott IC, Babakhanlou-Chase H, Palamakumbura AH, Pappano WN, Hong HH, Greenspan DS, Trackman PC. Multiple bone morphogenetic protein 1-related mammalian metalloproteinases process pro-lysyl oxidase at the correct physiological site and control lysyl oxidase activation in mouse embryo fibroblast cultures. *J Biol Chem* 2001; **276**:22537–22543.
12. Zhou Y, Ling O, Bo L. Expression and significance of lysyl oxidase-like 1 and fibulin-5 in the cardinal ligament tissue of patients with pelvic floor dysfunction. *J Biomed Res* 2013; **27**:23–28.
13. Klutke J, Ji Q, Campeau J, Starcher B, Felix JC, Stanczyk FZ, Klutke C. Decreased endopelvic fascia elastin content in uterine prolapse. *Acta Obstet Gynecol Scand* 2008; **87**:111–115.
14. Jung HJ, Jeon MJ, Yim GW, Kim SK, Choi JR, Bai SW. Changes in expression of fibulin-5 and lysyl oxidase-like 1 associated with pelvic organ prolapse. *Eur J Obstet Gynecol Reprod Biol* 2009; **145**:117–122.
15. Alarab M, Bortolini MA, Drutz H, Lye S, Shynlova O. LOX family enzymes expression in vaginal tissue of premenopausal women with severe pelvic organ prolapse. *Int Urogynecol J* 2010; **21**:1397–1404.
16. Zhao BH, Zhou JH. Decreased expression of elastin, fibulin-5 and lysyl oxidase-like 1 in the uterosacral ligaments of postmenopausal women with pelvic organ prolapse. *J Obstet Gynaecol Res* 2012; **38**:925–931.
17. Kow N, Ridgeway B, Kuang M, Butler RS, Damaser MS. Vaginal expression of LOXL1 in premenopausal and postmenopausal women with pelvic organ prolapse. *Female Pelvic Med Reconstr Surg* 2016; **22**: 229–235.
18. Liu X, Zhao Y, Gao J, Pawlyk B, Starcher B, Spencer JA, Yanagisawa H, Zuo J, Li T. Elastic fiber homeostasis requires lysyl oxidase-like 1 protein. *Nat Genet* 2004; **36**:178–182.
19. Alperin M, Debes K, Abramowitch S, Meyn L, Moalli PA. LOXL1 deficiency negatively impacts the biomechanical properties of the mouse vagina and supportive tissues. *Int Urogynecol J Pelvic Floor Dysfunct* 2008; **19**:977–986.
20. Wieslander CK, Rahn DD, McIntire DD, Acevedo JF, Drewes PG, Yanagisawa H, Word RA. Quantification of pelvic organ prolapse in mice: vaginal protease activity precedes increased MOPQ scores in fibulin 5 knockout mice. *Biol Reprod* 2009; **80**:407–414.
21. Lee UJ, Gustilo-Ashby AM, Daneshgari F, Kuang M, Vurbic D, Lin DL, Flask CA, Li T, Damaser MS. Lower urogenital tract anatomical and functional phenotype in lysyl oxidase like-1 knockout mice resembles female pelvic floor dysfunction in humans. *Am J Physiol Renal Physiol* 2008; **295**:F545–F555.
22. Hendrix SL, Clark A, Nygaard I, Aragaki A, Barnabei V, McTiernan A. Pelvic organ prolapse in the Women's Health Initiative: gravity and gravidity. *Am J Obstet Gynecol* 2002; **186**:1160–1166.
23. Borazjani A, Pizarro-Berdichevsky J, Goldman HB, Damaser MS. *Successive increases in parity conver a significant increase in risk for pelvic organ prolapse in mice and women*. Cape Town, South Africa: International Urogynecological Association; 2016.
24. Gustilo-Ashby AM, Lee U, Vurbic D, Sypert D, Kuang M, Daneshgari F, Barber MD, Damaser MS. The impact of cesarean delivery on pelvic floor dysfunction in lysyl oxidase like-1 knockout mice. *Female Pelvic Med Reconstr Surg* 2010; **16**:21–30.
25. Fritel X, Ringa V, Varnoux N, Fauconnier A, Piault S, Breart G. Mode of delivery and severe stress incontinence. A cross-sectional study among 2,625 perimenopausal women. *BJOG* 2005; **112**:1646–1651.

26. Borazjani A, Kow N, Harris S, Ridgeway B, Damaser MS. Transcriptional regulation of connective tissue metabolism genes in women with pelvic organ prolapse. *Female Pelvic Med Reconstr Surg* 2017; **23**:44–52.
27. Fisher RA. On the probable error of a coefficient of correlation deduced from a small sample. *Metro* 1921; **1**:3–32.
28. Kleinbaum DG, Kupper LL. *Applied Regression Analysis and Other Multivariable Methods*. Boston, MA: Cengage Learning; 2014: 257–267.
29. Motulsky HJ, Brown RE. Detecting outliers when fitting data with nonlinear regression - a new method based on robust nonlinear regression and the false discovery rate. *BMC Bioinformatics* 2006; **7**:123.
30. Sze EH, Sherard GB III, Dolezal JM. Pregnancy, labor, delivery, and pelvic organ prolapse. *Obstet Gynecol* 2002; **100**:981–986.
31. Wieslander CK, Marinis SI, Drewes PG, Keller PW, Acevedo JF, Word RA. Regulation of elastolytic proteases in the mouse vagina during pregnancy, parturition, and puerperium. *Biol Reprod* 2008; **78**:521–528.
32. Daucher JA, Clark KA, Stolz DB, Meyn LA, Moalli PA. Adaptations of the rat vagina in pregnancy to accommodate delivery. *Obstet Gynecol* 2007; **109**:128–135.
33. Oliphant SS, Nygaard IE, Zong W, Canavan TP, Moalli PA. Maternal adaptations in preparation for parturition predict uncomplicated spontaneous delivery outcome. *Am J Obstet Gynecol* 2014; **211**:630 e631–637.
34. Shynlova O, Bortolini MA, Alarab M. Genes responsible for vaginal extracellular matrix metabolism are modulated by women's reproductive cycle and menopause. *Int Braz J Urol* 2013; **39**:257–267.
35. Kerkhof MH, Hendriks L, Brolmann HA. Changes in connective tissue in patients with pelvic organ prolapse–a review of the current literature. *Int Urogynecol J Pelvic Floor Dysfunct* 2009; **20**:461–474.
36. Drewes PG, Yanagisawa H, Starcher B, Hornstra I, Csiszar K, Marinis SI, Keller P, Word RA. Pelvic organ prolapse in fibulin-5 knockout mice: pregnancy-induced changes in elastic fiber homeostasis in mouse vagina. *Am J Pathol* 2007; **170**:578–589.
37. Liu X, Zhao Y, Pawlyk B, Damaser M, Li T. Failure of elastic fiber homeostasis leads to pelvic floor disorders. *Am J Pathol* 2006; **168**:519–528.
38. Li SW, Sieron AL, Fertala A, Hojima Y, Arnold WV, Prockop DJ. The C-proteinase that processes procollagens to fibrillar collagens is identical to the protein previously identified as bone morphogenic protein-1. *Proc Natl Acad Sci U S A* 1996; **93**:5127–5130.
39. Kessler E, Takahara K, Biniaminov L, Brusel M, Greenspan DS. Bone morphogenetic protein-1: the type I procollagen C-proteinase. *Science* 1996; **271**:360–362.
40. Zeisberg M, Strutz F, Muller GA. Role of fibroblast activation in inducing interstitial fibrosis. *J Nephrol* 2000; **13** Suppl 3:S111–120.
41. Kalluri R, Zeisberg M. Fibroblasts in cancer. *Nat Rev Cancer* 2006; **6**:392–401.
42. Rodemann HP, Muller GA. Characterization of human renal fibroblasts in health and disease: II. In vitro growth, differentiation, and collagen synthesis of fibroblasts from kidneys with interstitial fibrosis. *Am J Kidney Dis* 1991; **17**:684–686.
43. Hung CF, Rohani MG, Lee SS, Chen P, Schnapp LM. Role of IGF-1 pathway in lung fibroblast activation. *Respir Res* 2013; **14**:102.
44. Pang M, Ma L, Gong R, Tolbert E, Mao H, Ponnusamy M, Chin YE, Yan H, Dworkin LD, Zhuang S. A novel STAT3 inhibitor, S3I-201, attenuates renal interstitial fibroblast activation and interstitial fibrosis in obstructive nephropathy. *Kidney Int* 2010; **78**:257–268.
45. Stanczyk J, Ospelt C, Karouzakis E, Filer A, Raza K, Kolling C, Gay R, Buckley CD, Tak PP, Gay S, Kyburz D. Altered expression of microRNA-203 in rheumatoid arthritis synovial fibroblasts and its role in fibroblast activation. *Arthritis Rheum* 2011; **63**:373–381.
46. Latham N, Mason G. From house mouse to mouse house: the behavioural biology of free-living Mus musculus and its implications in the laboratory. *Appl Anim Behav Sci* 2004; **86**:261–289.
47. Curley JP, Jordan ER, Swaney WT, Izraelit A, Kammel S, Champagne FA. The meaning of weaning: influence of the weaning period on behavioral development in mice. *Dev Neurosci* 2009; **31**:318–331.
48. Zong W, Stein SE, Starcher B, Meyn LA, Moalli PA. Alteration of vaginal elastin metabolism in women with pelvic organ prolapse. *Obstet Gynecol* 2010; **115**:953–961.
49. Moalli PA, Shand SH, Zyczynski HM, Gordy SC, Meyn LA. Remodeling of vaginal connective tissue in patients with prolapse. *Obstet Gynecol* 2005; **106**:953–963.
50. Almudevar A, Klebanov LB, Qiu X, Salzman P, Yakovlev AY. Utility of correlation measures in analysis of gene expression. *NeuroRx* 2006; **3**:384–395.
51. Reynier F, Petit F, Paye M, Turrel-Davin F, Imbert P-E, Hot A, Mougin B, Miossec P. Importance of correlation between gene expression levels: application to the type I interferon signature in rheumatoid arthritis. *PLoS One* 2011; **6**:e24828.
52. Weirauch MT. Gene Coexpression Networks for the Analysis of DNA Microarray Data. In: *Applied Statistics for Network Biology*. Wiley-VCH Verlag GmbH & Co. KGaA; 2011: 215–250.
53. Herschorn S. Female pelvic floor anatomy: the pelvic floor, supporting structures, and pelvic organs. *Rev Urol* 2004; **6** Suppl 5:S2-s10.
54. Maquart FX, Simeon A, Pasco S, Monboisse JC. Regulation of cell activity by the extracellular matrix: the concept of matrikines. *J Soc Biol* 1999; **193**:423–428.
55. Simeon A, Monier F, Emonard H, Wegrowski Y, Bellon G, Monboisse JC, Gillery P, Hornebeck W, Maquart FX. Fibroblast-cytokine-extracellular matrix interactions in wound repair. *Curr Top Pathol* 1999; **93**: 95–101.
56. Blanchevoye C, Floquet N, Scandolera A, Baud S, Maurice P, Bocquet O, Blaise S, Ghoneim C, Cantarelli B, Delacoux F, Dauchez M, Efremov RG et al. Interaction between the elastin peptide VGVAPG and human elastin binding protein. *J Biol Chem* 2013; **288**:1317–1328.
57. Brassart B, Fuchs P, Huet E, Alix AJ, Wallach J, Tamburro AM, Delacoux F, Haye B, Emonard H, Hornebeck W, Debelle L. Conformational dependence of collagenase (matrix metalloproteinase-1) up-regulation by elastin peptides in cultured fibroblasts. *J Biol Chem* 2001; **276**: 5222–5227.
58. Wells JM, Gaggar A, Blalock JE. MMP generated matrikines. *Matrix Biol* 2015; **44**:122–129.
59. Maquart FX, Pickart L, Laurent M, Gillery P, Monboisse JC, Borel JP. Stimulation of collagen synthesis in fibroblast cultures by the tripeptide-copper complex glycyl-L-histidyl-L-lysine-Cu2+. *FEBS Lett* 1988; **238**:343–346.
60. Wachi H, Seyama Y, Yamashita S, Suganami H, Uemura Y, Okamoto K, Yamada H, Tajima S. Stimulation of cell proliferation and autoregulation of elastin expression by elastin peptide VPGVG in cultured chick vascular smooth muscle cells. *FEBS Lett* 1995; **368**:215–219.
61. Gaggar A, Jackson PL, Noerager BD, O'Reilly PJ, McQuaid DB, Rowe SM, Clancy JP, Blalock JE. A novel proteolytic cascade generates an extracellular matrix-derived chemoattractant in chronic neutrophilic inflammation. *J Immunol* 2008; **180**:5662–5669.
62. Senior RM, Griffin GL, Mecham RP, Wrenn DS, Prasad KU, Urry DW. Val-Gly-Val-Ala-pro-Gly, a repeating peptide in elastin, is chemotactic for fibroblasts and monocytes. *J Cell Biol* 1984; **99**: 870–874.